

Cryoprinting of Functional Hydrogels

Nivedita Chandra Bose

1 Introduction

1.1 3D Multimaterial Cryoprinting

Three-dimensional extrusion-based bioprinting has become a key technology for creating 3D biological constructs using biocompatible materials such as biomaterials, cells, and bioactive molecules. A new subset of this technology, called cryoprinting, involves depositing layers of material onto a cryoplate kept at temperatures below 0°C . As the material touches the cryoplate, it freezes, forming 3D structures. This process is illustrated in Figures 1a and 1b. Cryoprinting allows for the simultaneous printing of different materials and is especially effective for printing low-viscosity materials, which are usually difficult to handle. Potential applications of this technique include tissue engineering, bioelectronics, and regenerative medicine.

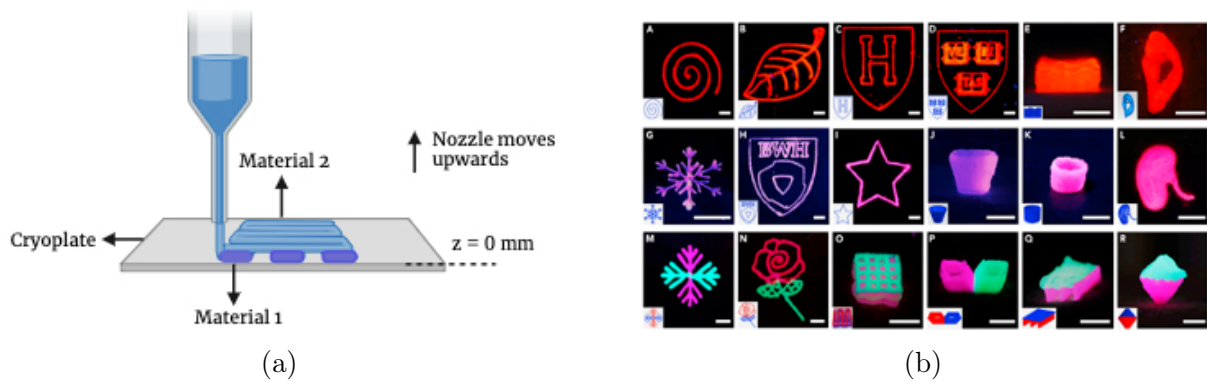


Figure 1: (a) Schematic of multi-material 3D cryoprinting. (b) Cryoprinted structures of single and multiple materials [1].

1.2 Biopotential monitoring

Cryoprinting can potentially be used to fabricate biopotential monitoring devices. Biopotential monitoring involves measuring and recording the body's electrical signals to understand the physiological functions of organs such as the heart, brain, and muscles. For example, electrocardiography (ECG) measures the electrical signals of the heart, and electroencephalography (EEG) monitors the electrical activity in the brain.

1.3 Hydrogels

Hydrogels are 3D flexible, water-absorbent polymers that can be used in biopotential monitoring devices. They are already widely used in many biomedical applications due

to their biocompatibility and strong adhesion, as shown in Figure 2. Hydrogels undergo cross-linking or gelation through chemical or physical processes to become stiffer.

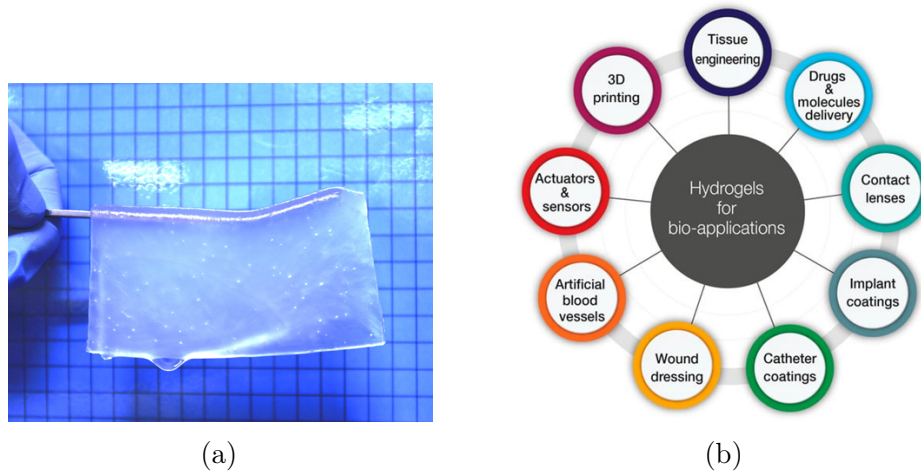


Figure 2: (a) Semi-transparent hydrogel [2]. (b) Applications of hydrogels in biomedicine [3].

1.4 Alginate-based hydrogel and PEDOT:PSS

Alginate-based hydrogel (AH) shows promise for these devices due to its tissue-mimicking behavior, good shape conformity, ease of processing, and high compatibility with PEDOT:PSS, a conductive material that enhances signal quality. AH can be cross-linked with calcium ions using solutions such as calcium chloride.

PEDOT:PSS (Poly(3,4-ethylenedioxythiophene) polystyrene sulfonate) is ideal for biopotential monitoring due to its low contact impedance, biocompatibility, and adjustable electrical properties. Unlike traditional metal electrodes, it conforms better to body shapes. Adding dimethyl sulfoxide (DMSO) can increase its viscosity.

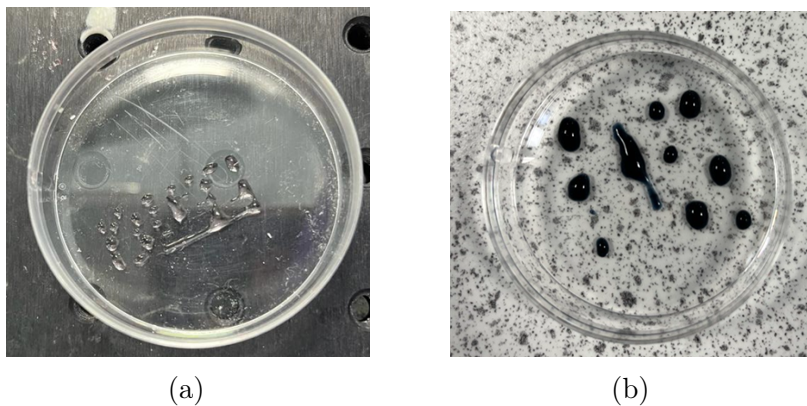


Figure 3: (a) Attempts at 3D extrusion printing of 4% AH grid. (b) Attempts at 3D extrusion printing of PEDOT:PSS grid.

However, AH and PEDOT:PSS have low viscosity which makes it hard to manufacture

and print such devices as demonstrated in Figure 3. Additionally, challenges remain in scaling up the fabrication of these monitoring constructs and improving signal quality.

2 Project Aims and Goals

This project explores the development and evaluation of an innovative cryoprinting method for fabricating AH and 5% DMSO PEDOT:PSS constructs for biopotential monitoring applications. By using multi-material 3D cryoprinting, the project aims to overcome the challenges of traditional 3D printing, such as difficulties in printing low-viscosity materials like AH and PEDOT:PSS.

3 Design of Cryoprinting Platform

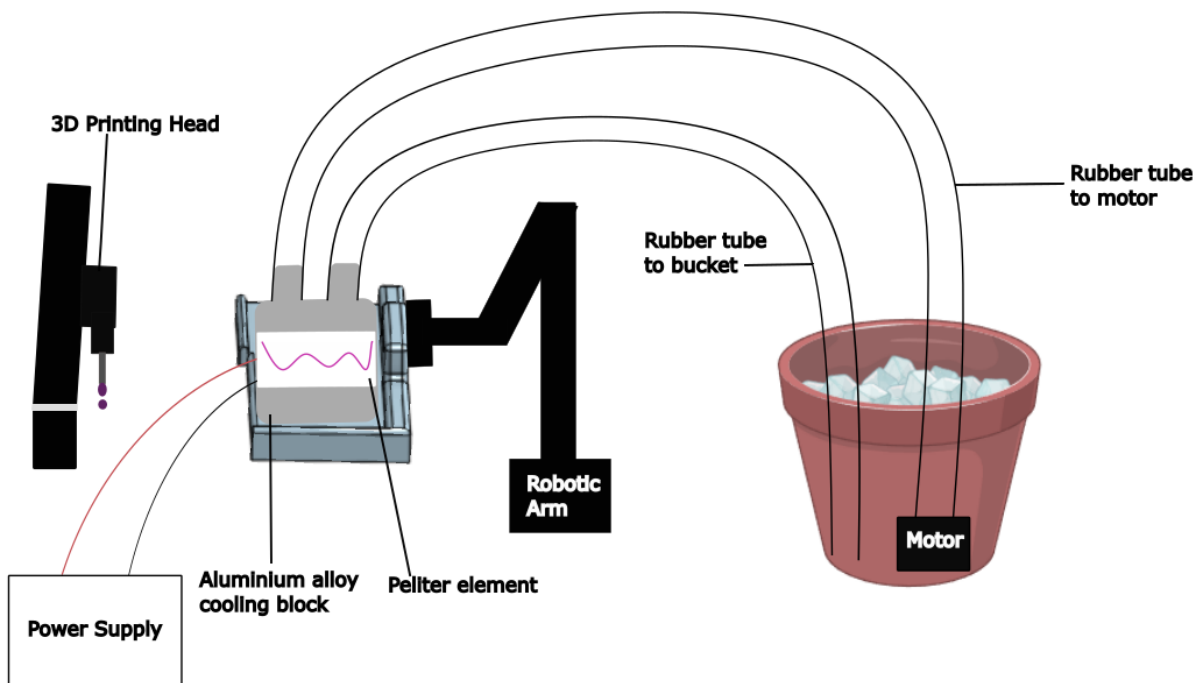


Figure 4: Schematic of the integrated cryoprinting platform setup.

A cryoprinting platform was developed (Figure 4) and integrated with the BioArm, an in-house 3D printer (Figure 5a). This platform uses a Peltier element to create a cryoplate for quickly solidifying extruded materials. The Peltier element generates a heat flux by converting electrical energy, resulting in one side becoming hot and the other side cool (Figure 5b). The hot side of the Peltier element is attached to an aluminium cooling block, which circulates ice-cold water using a motor to prevent overheating.

Multi-layered constructs composed of 10% gelatin, 4% AH, and PEDOT:PSS were successfully cryoprinted, demonstrating the platform's viability for printing 3D structures.

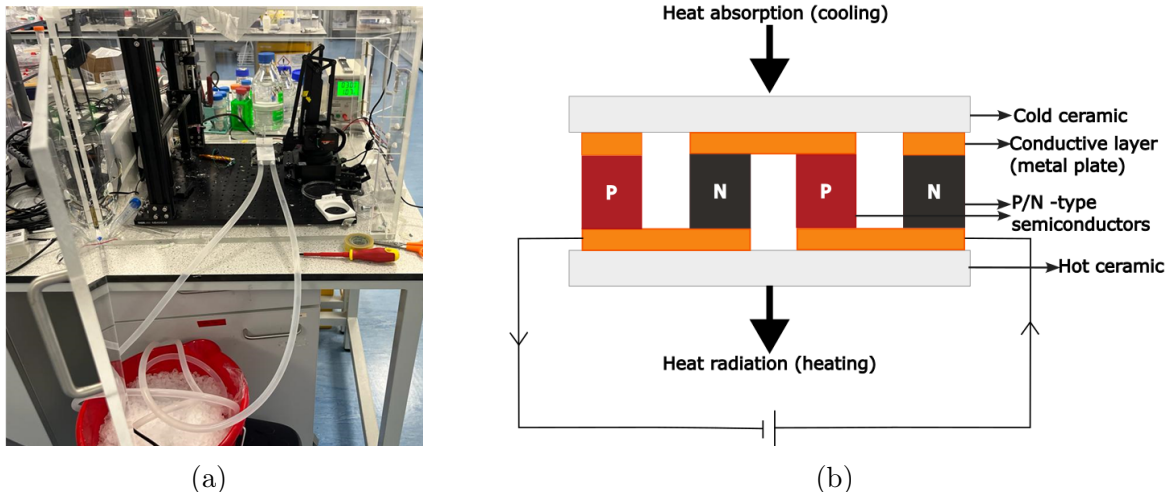


Figure 5: (a) Assembly of the integrated cryoprinting platform. (b) Peltier element module structure.

Temperature characterisations of the cryoprinting platform confirmed its functionality for fabricating these structures. However, the process encountered limitations due to the premature freezing of extruded materials. These issues were optimised by adjusting printing parameters such as voltage, printing speed, delay time, layer height, step size, and nozzle size.

4 Cryoprinting AH

AH was successfully cryoprinted and cross-linked using CaCl_2 , shown in Figure 6. However, the process encountered several challenges, such as supercooling, which led to bead-like structures, premature freezing, and potential non-uniform cross-linking. These issues caused errors in the print and distortion.

Despite these challenges, tests were conducted to compare theoretical measurements and those taken before and after cross-linking. These tests included:

1. Lateral Pore Test: Used to compare the theoretical and cryoprinted and cross-linked internal pore area of 30 x 10 mm grids.
2. Filament Width Test: Assessed the differences between the widths of cryoprinted lines and the theoretical values.
3. Filament Fusion Test: Measured spreadability using square waves of decreasing spacing.

The results indicated good shape fidelity and precision. However, improvements in the cross-linking and drying processes are necessary to minimize structural distortion.

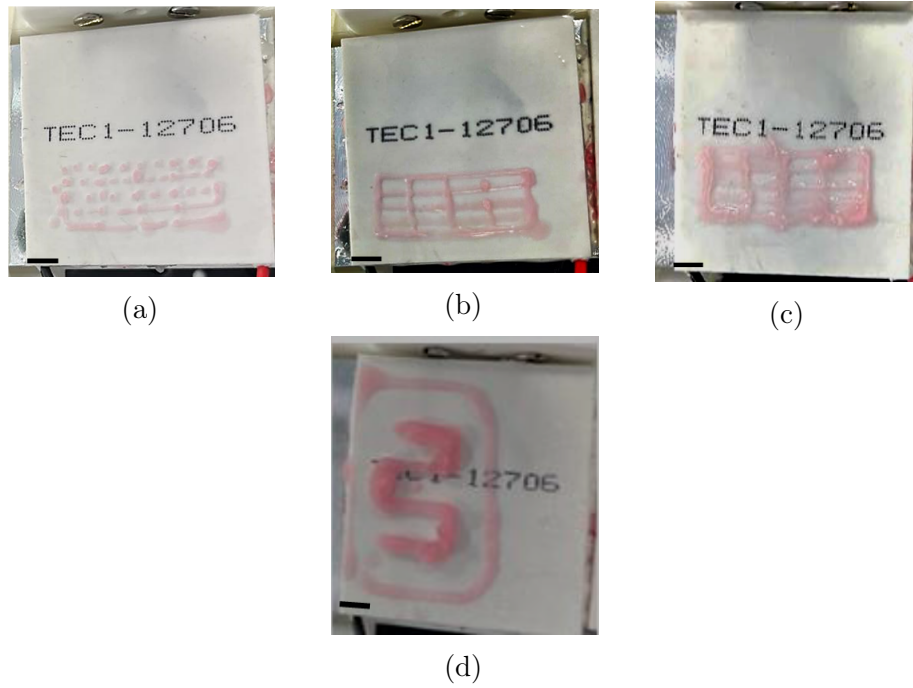


Figure 6: (a) Inconsistent 4% AH cryoprint using parameters optimised for gelatine. (b) 4% AH cryoprinted 30 mm x 10 mm grid for calibration and lateral pore test. (c) 4% AH grid from (b) cross-linked with 140 mM CaCl_2 . (d) 10-layer cryoprinted 4% AH square wave. All scale bars are 5mm.

5 Cryoprinting PEDOT:PSS

PEDOT:PSS was successfully cryoprinted, demonstrating a novel approach with good printability, resolution, and shape fidelity, as depicted in Figure 7. The cryoprinted PEDOT:PSS structures could not hold their shape after thawing, as shown in Figure 8, indicating the need for additives to ensure structural integrity.

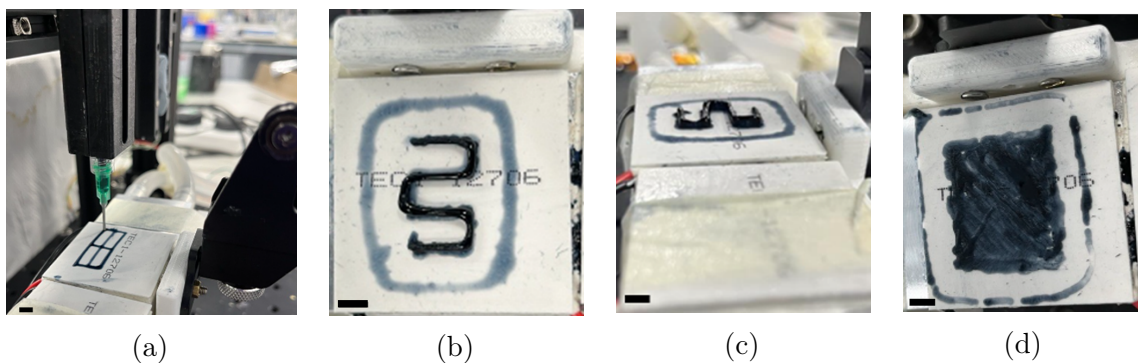


Figure 7: (a) Cryoprinting of a 2x2 PEDOT:PSS grid structure. (b) Cryoprinting of a square wave pattern. (c) Side view of a 10-layer square wave pattern cryoprint. (d) Cryoprint of a 1-layer square. All scale bars are 5 mm.

5% DMSO was added to PEDOT:PSS as it is biocompatible and can enhance electrical properties and structural integrity. The addition of 5% DMSO to PEDOT:PSS improved the processability, leading to better extrusion and more uniform filament dimensions,

demonstrated in Figure 9. Cryoprinted 5% DMSO PEDOT:PSS lines maintained their shape more effectively after thawing and exhibited significantly higher conductivity, approximately 58.6% higher (Table 10) than 3D-printed lines, most likely due to the enhanced alignment and orientation of PEDOT chains during rapid freezing. Although the printability of cryoprinted PEDOT:PSS was only slightly improved, the enhancement in conductivity is crucial for creating biopotential monitoring patches with higher signal acquisition, better conductivity, and sensitivity.



Figure 8: (a) Cryoprinted 5-layer square wave structure before thawing. (b) Cryoprinted 5-layer square wave structure after thawing. All scale bars represent 5 mm.

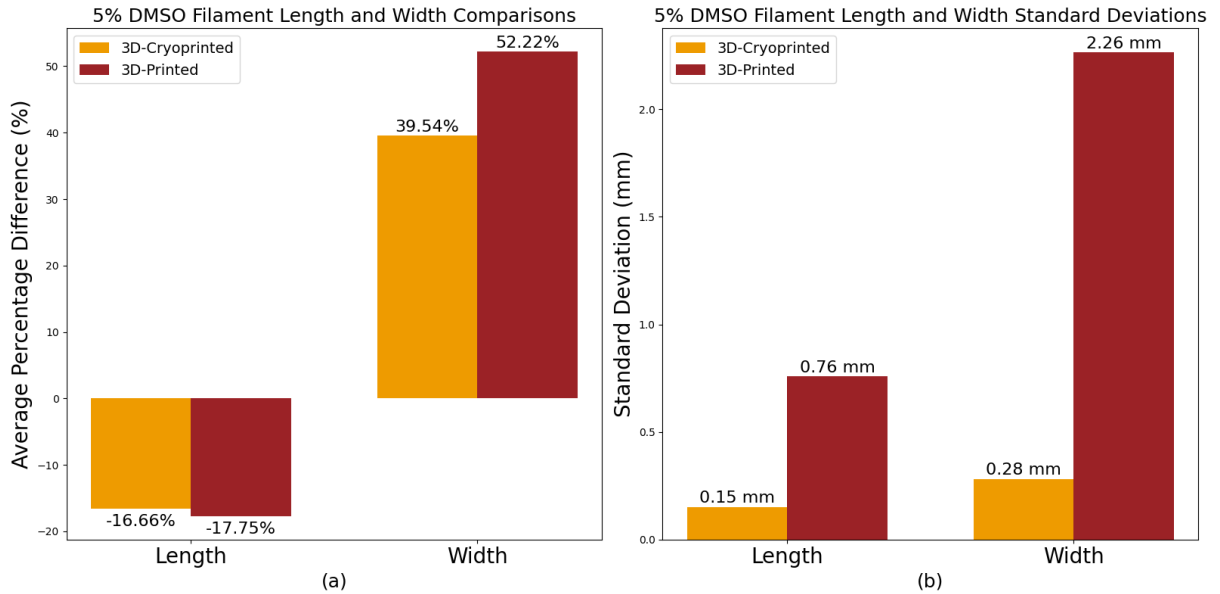


Figure 9: (a) Filament length and width comparisons for cryoprinted and printed 5% DMSO PEDOT:PSS. (b) Filament length and width standard deviations for cryoprinted and printed 5% DMSO PEDOT:PSS.

Method	Average Conductivity (S/m)	Standard Deviation (S/m)
3D-Cryoprinted	330.8	146.3
3D-Printed	208.6	83.1

Figure 10: Comparison of Average Conductivity and Standard Deviation between 3D-Cryoprinted and 3D-Printed Methods

6 Developing Integrated PEDOT:PSS and AH Constructs

Integrated PEDOT:PSS and AH structures were successfully cryoprinted (Figure 11) and tested for electrical properties by overlapping AH and PEDOT:PSS layers (Figure 12).

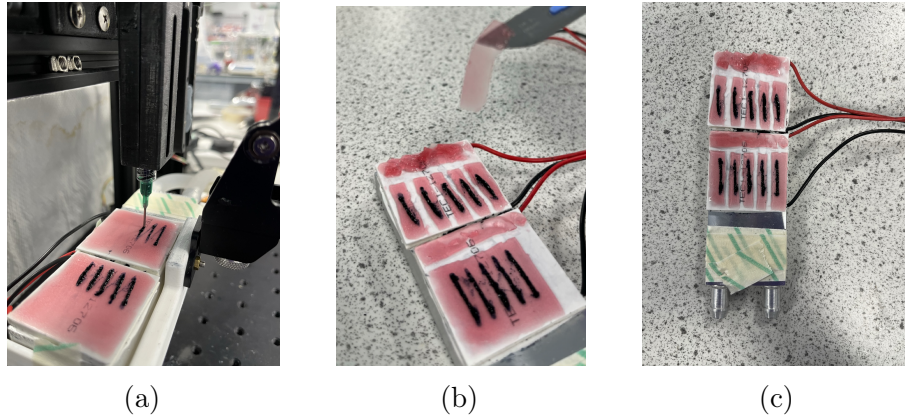


Figure 11: (a) Cryoprinting 5% DMSO PEDOT:PSS lines on cryoprinted and cross-linked AH. (b) Separation of the lines into rectangular slabs using a scalpel. (c) Separated lines left to dry overnight.

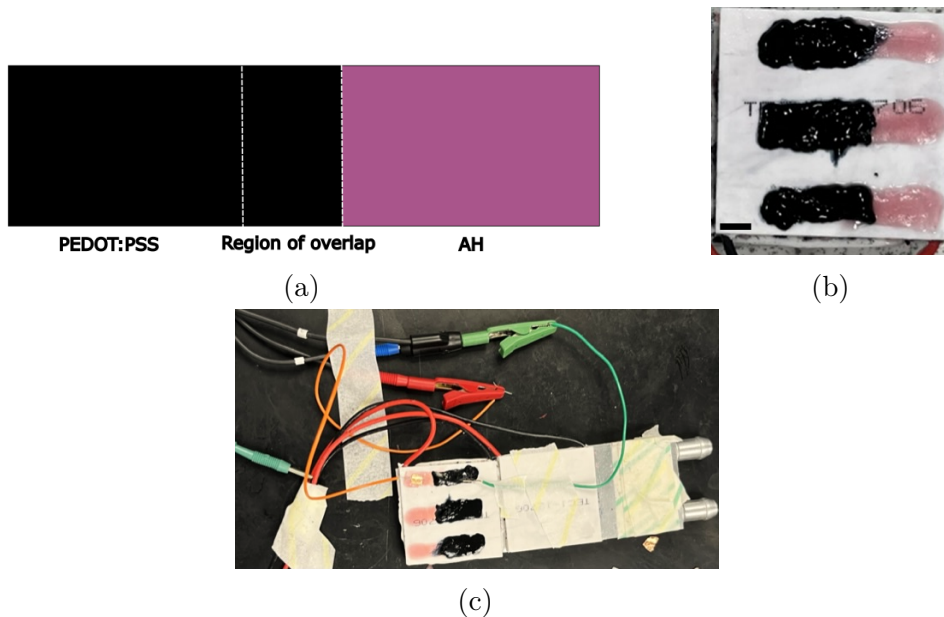


Figure 12: (a) Model for the PEDOT:PSS-AH constructs with a region of overlap. (b) Five cryoprinted rectangles of 5% DMSO PEDOT:PSS and cross-linked AH with a region of overlap. The scale bar represents 5mm. (c) Connections of the PalmSens neutral and measuring electrodes to the construct via copper wires and tape.

The constructs exhibited higher impedances compared to values reported in the literature. However, the introduction of 5% DMSO and the use of cryoprinting significantly improved

conductivity over traditional 3D printing methods and pure PEDOT:PSS, as shown in Figure 13. Despite these improvements, challenges persist in achieving reliable electrical connections and low impedance when integrating cryoprinted PEDOT:PSS with AH constructs. This difficulty may stem from poor adhesion between the two materials.

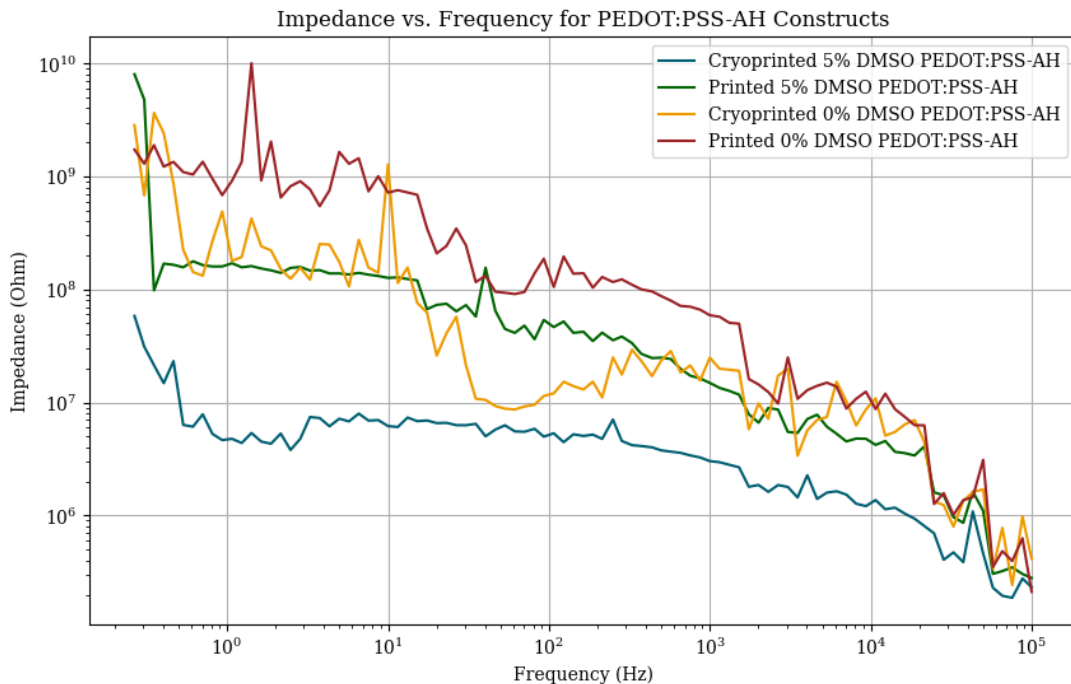


Figure 13: Impedance vs. frequency plot for cryoprinted and printed PEDOT:PSS-AH constructs with 0% and 5% DMSO concentrations.

The study also underscores the potential of cryoprinting for producing 3D structures with excellent resolution and minimal material wastage, indicating promise for scalability and speed. Nonetheless, successful implementation requires materials compatible with low temperatures and modifications in ink formulation to fully realize this technology’s potential.

7 Conclusion

This project has demonstrated the potential of cryoprinting in fabricating biopotential monitoring constructs, particularly through the use of conductive PEDOT:PSS-AH structures enhanced with DMSO. The technique offers improvements in printability, structural integrity, and electrical performance, indicating its suitability for developing intricate and reliable biopotential monitoring devices. However, further work is needed to refine ink formulations, enhance the adhesion of constructs, and reduce impedance. Addressing these challenges will be crucial for optimising the process and expanding the application of cryoprinting in biopotential monitoring and other bioelectronics fields.

References

- [1] Hossein Ravanbakhsh et al. “Freeform cell-laden cryobioprinting for shelf-ready tissue fabrication and storage”. In: *Matter* 5.2 (2022), pp. 573–593.
- [2] Satoshi Tanikawa et al. “Engineering of an electrically charged hydrogel implanted into a traumatic brain injury model for stepwise neuronal tissue reconstruction”. In: *Scientific reports* 13.1 (2023), p. 2233.
- [3] Oliwia Kapusta et al. “Antimicrobial natural hydrogels in biomedicine: Properties, Applications, and challenges—A concise review”. In: *International Journal of Molecular Sciences* 24.3 (2023), p. 2191.